Pergamon

Tetrahedron, Vol. 53, No. 37, pp. 12377-12390, 1997

0040-4020/97 $17.00 + 0.00

PII: S0040-4020(97)00800-4

Synthesis, Electronic and ^{1}H NMR Properties of a New Type of Polypyridyl Ligand: Long-Range Ring Current Effects

Youxiang Wang and D. Paul Rillema*

Department of Chemistry, Wichita State University, Wichita, KS 67260-0051

Abstract: The preparation of a series of heterocycles obtained by the condensation of 4,5-diazafluoren-9-one with various amines is described with particular emphasis on bridged systems formed by the condensation of 4,5-diazafluoren-9-one with diamine compounds such as hydrazine. Due to sp^2 hybridization of the nitrogen atom in the bridge, the protons in the two pyridine units of each bipyridine group are non-equivalent. The projection of a hydrogen atom from one of the pyridine rings into the ring current of an adjacent phenyl ring shifts the proton resonance upfield. Proton NMR resonances have been uniquely assigned for all the compounds and electronic absorptions have been attributed to $\pi \rightarrow \pi^*$ transitions located in the ultraviolet region of the spectrum. Reduction of the heterocycles occurs at the imine nitrogen bridge and is irreversible, except for the ligand resulting from the condensation of 4,5-diazafluoren-9-one with hydrazine. © 1997 Elsevier Science Ltd.

INTRODUCTION

One of the main goals of molecular electronics is the mastery of intramolecular electron transfer over long distances[1]. This requires the assembly of suitable molecular components into an appropriate supramolecular

structure[2]. Polypyridyl ruthenium(II) complexes are excellent building blocks for the construction of such devices[3] due to their photochemical properties and it is, therefore, not surprising that the number of investigations concerning the photochemical and photophysical behavior of dinuclear or polynuclear complexes of this type is rapidly growing[4]. Key components of polynuclear complexes are the bridging ligands, since the interactions between the units and thereby, the properties of the polynuclear complexes are critically dependent on the size, shape, and electronic nature of the bridge. Such bridging ligands allow the preparation of polynuclear complexes in which long-range metal-metal interactions in all their forms may be studied, such as optical electron-transfer in mixed valence species[5], photoinduced electron transfer or energy transfer between an excited-state chromophore and a quencher[6], and magnetic exchange between paramagnetic centers[7]. The knowledge gained from energy and electron transfer in bimetallic systems has led us to synthesize new ligand systems (Figure 1). Such ligands demonstrate: (i) a large variable length allowing connection to metal complexes at variable distances; (ii) conjugated character to explore efficient electron or energy transfer; and (iii) a rigid structure to avoid rotational conformation problems.

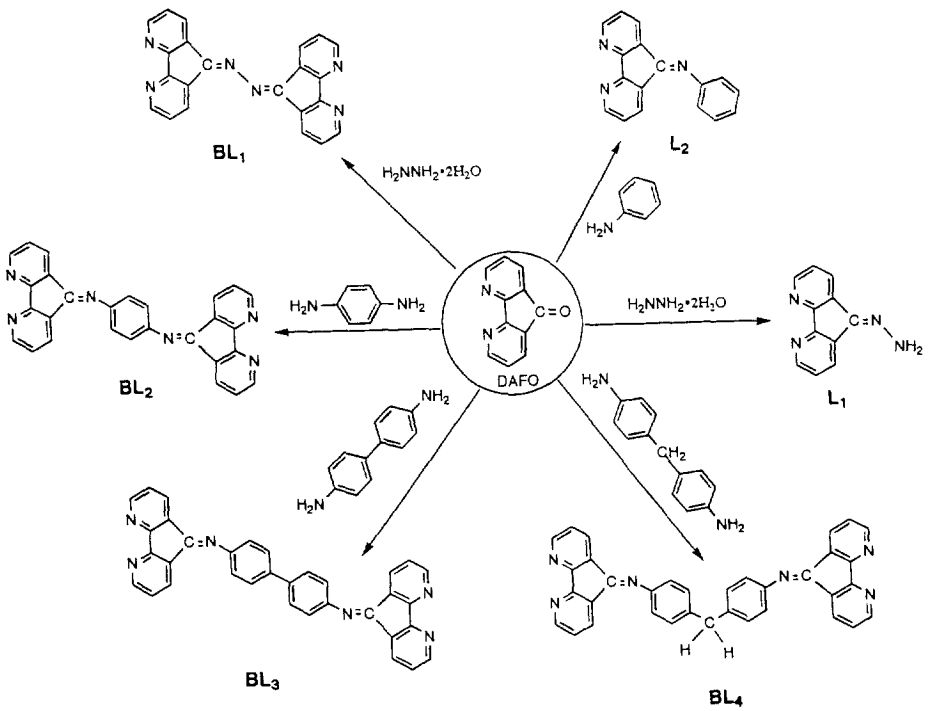

Figure 1. Structures of ligands.

RESULTS AND DISCUSSION

Synthesis of Ligands. Linking polypyridyl bridged ligands, such as 2,2'-bipyridine or 1,10-phenanthroline, by C=C[8] or C-C[9] bonds is a difficult and tedious synthetic task. To circumvent this problem, we have turned our attention to a special ligand, 4,5-diazafluoren-9-one[10] which, in addition to having similar coordination properties as 2,2'-bipyridine, contains a reactive exocyclic ketone. This feature allows one to carry out condensation reactions between diazafluorenone and amines such as hydrazine, aniline, 1,4-diaminobenzene, benzidine or 4,4'-methylenedianiline. Incorporation of nitrogen atoms into the bridge forming the CH=N group, which is isoelectronic with the CH=CH group, is another approach to synthesize polypyridyl bridged ligands.

Various Lewis acids such as zinc chloride, aluminum chloride, glacial acetic acid, phenol or trifluoroacetic acid, have been used to catalyze reactions of this type. Our experiments have shown that glacial acetic acid served our purpose best. It acted both as the solvent and the catalyst. Furthermore, the products were not soluble in it and readily precipitated out of the solution.

The reaction time was very important regardless of the catalyst used. If the reaction was longer than one hour with zinc chloride or aluminum chloride as a catalyst, an oily product was formed in substantial amount. When the catalyst was glacial acetic acid, the desired product was formed very rapidly, but, gradually decomposed if the refluxing time was too long.

The solubility of the ligands is related to intramolecular forces, intermolecular forces and the molecular structure. The order of solubility was $BL_4 > BL_1 > BL_3 > BL_2$. Asymmetry in the compounds was introduced by way of hybridization about the bridge nitrogen atom and rotations about the phenyl rings and methylene spacer. BL_4 is the most distorted, hence the most soluble. It was followed by BL_1 which is less conjugated than BL_2 and BL_3. The additional rotation freedom in BL_3 resulted in greater solubility than found for BL_2.

Mass Spectra of the Ligands. Mass spectral data were collected for all the ligands and the data are listed in Table 1. The relative abundances of parent molecular ion peaks for BL_2, BL_1, BL_3 and BL_4, where the highest peak in a given map was assigned a value of 100 and the other peak heights were compared to it, were 100, 66.8, 4.7, 0.6, respectively and reflect the relative stability of the four ligands in the gas phase. In general, the larger the molecule, the less stable it becomes in the gas phase, although BL_2 is more stable than BL_1, presumably due to its more extensive π conjugation. BL_4 generated the molecular ion peak of BL_1; BL_3

Table 1. Mass Spectroscopy Analysis of Bridged Ligands BL_{1-4}

BL_1 MW= 360		BL_2 MW= 436		BL_3 MW= 512		BL_4 MW= 526	
Mass Charge ratio	Relative Abundance	Mass Charge ratio	Relative Abundance	Mass Charge ratio	Relative Abundance	Mass Charge ratio	Relative Abundance
360	**66.8**	**436**	**100**	**512**	**4.7**	**526**	**0.6**
331	20.8	272	5.6	**436**	**100**	**360**	**1.1**
257	14.7	218	3.3	256	5.3	156	15.3
181	25.6	77	8.9	218	10.1	126	6.0
154	19.1			149	5.8	82	12.8
126	23.1			91	5.3		
103	13.2						
82	20.0						
57	25.9						

generated the molecular ion peak of BL_2 with a relative abundance of 100, showing the greater stability of the BL_2 ligand.

^{1}H NMR of Ligands. The ^{1}H NMR spectra of all the ligands, except for BL_2 due to its poor solubility in common NMR solvents were obtained and representative examples are shown in Figure 2. Proton assignments were made using H,H-COSY spectra, NOE spectra, and coupling/decoupling C-13 spectra. As shown for BL_1, the protons in the two pyridine rings of the bipyridine ligands are not equivalent because of sp^2 hybridization of the nitrogen atoms in the bridge. The chemical shifts for the α, β and γ protons are 8.82, 7.45, and 8.36 ppm, respectively; the chemical shifts for the α', β' and γ' protons are 8.77, 7.32, and 8.52 ppm, respectively. The difference in the chemical shifts of α and α', β and β', γ and γ' can be related to two effects. The first, or primary effect, is related to the interaction of the α, β, γ and α', β', γ' protons with the lone pair on the θ nitrogen. The α, β, γ protons in the ring closer to the θ nitrogen lone pair are shifted upfield, whereas the α', β', γ' protons in the ring further from the θ nitrogen lone pair are shifted downfield, which is consistent with the literature[11]. The second effect is related to their interaction with the lone pair of the ϕ nitrogen. In this case an additional upfield contribution due to a paramagnetic shift of the α', β', γ' protons resulting from its interaction with the ϕ nitrogen (or, an intramolecular hydrogen bond) is likely, but an additional downfield

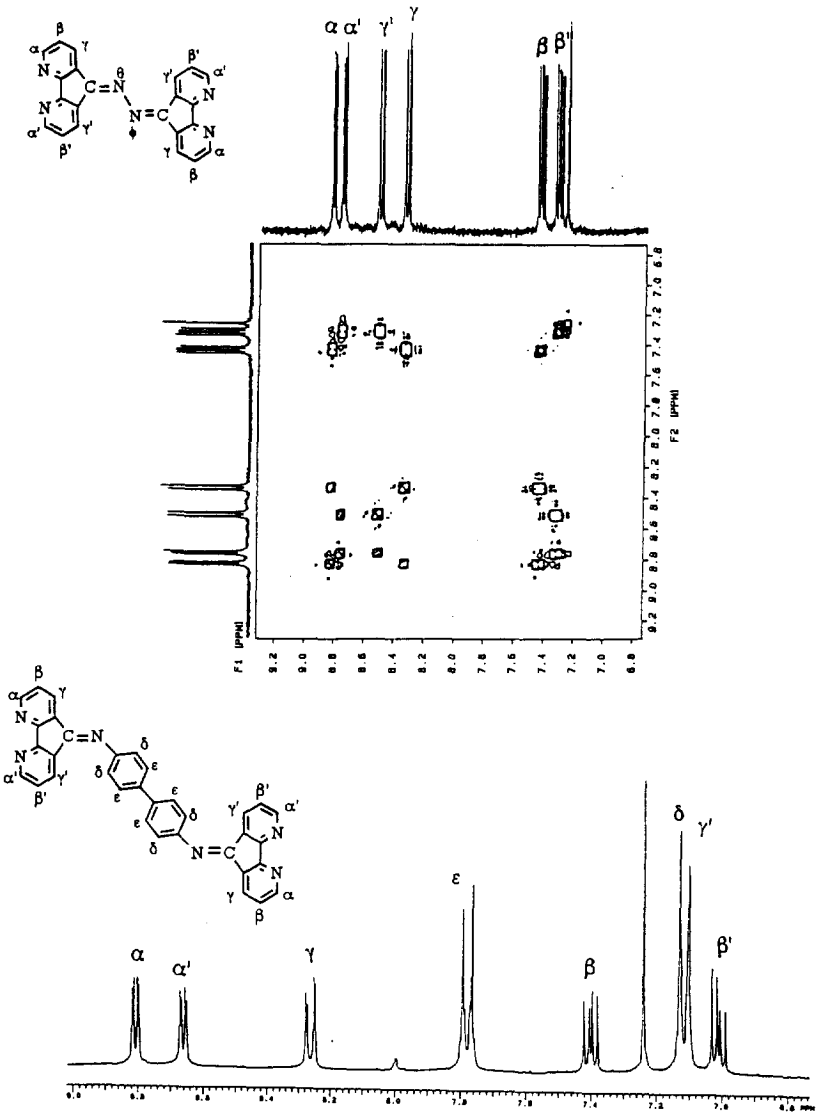

Figure 2. H,H-COSY spectrum of BL_1 (up) and ^1H NMR spectrum of BL_3 (down) in chloroform at room temperature.

contribution due to diamagnetic interaction of α, β, γ protons resulting from through C=N(θ) bond interaction is less likely[12]. The effect on the chemical shifts between the sets of protons (e.g., α and α', β and β', γ and γ') decreases in relation to their distance from the source of the effect.

The chemical shifts of biphenyl protons of BL_3 further prove the lone pair effect. Eight protons were divided into two groups. The δ protons closer to lone pair electrons have chemical shifts around 7.12 ppm and

the ε protons further from the lone pair electrons have chemical shifts around 7.78 ppm. The two groups of protons couple with each other resulting in a doublet. As shown in the spectrum, the γ (γ') and α (α') protons in reality are a doublet of doublets clearly showing long range coupling from the non-neighboring proton[13].

The chemical shifts of the γ' protons are very sensitive to the functional group attached to the bridged nitrogen. (γ' denotes protons ***cis*** to the substituent on the neighboring bridging nitrogen for all the ligands.) Table 2 summarizes the chemical shifts of γ and γ' protons for the various ligands. The six ligands are split into two groups based on chemical shift similarities of γ and γ' protons. The γ and γ' proton chemical shifts of BL_1, L_1 and L_3 belong to one group; the γ and γ' proton chemical shifts of BL_3, L_2 and BL_4 belong to the second group.

Table 2: γ and γ' Proton Chemical Shift of Ligands[a,b]

Ligands	γ Proton (ppm)	γ' Proton (ppm)
BL_1	8.36	8.52
L_1	8.18	8.59
L_3	8.03	8.65
BL_3	8.27	7.13
L_2	8.26	6.90
BL_4	8.22	7.31

a). Solvent: Chloroform.

b). BL_2 was not soluble enough in common NMR solvents to obtain a NMR spectrum.

The chemical shifts of γ protons do not change very much among the six ligands, but the chemical shift of γ' protons differ by 1.50 ppm between group one and group two protons. The difference results from long range ring current effects[10] due to the presence of phenyl components in the second group of compounds. The γ' protons sit right on top of the benzene ring in L_2, BL_3 and BL_4 as shown in Figure 3 for the structure of L_2 based on molecular modeling. Therefore, γ' protons are shifted about 1.50 ppm upfield. The distance of the γ' proton from the benzene ring of L_2, BL_3 and BL_4 and its chemical shift are also related. The distances of γ' protons to the benzene ring based on MM2 calculations are 2.56, 2.68 and 2.71 Å compared to chemical shifts of 6.90, 7.12 and 7.31 ppm, respectively. These shifts are similar to proton chemical shifts of [10]-paracyclophane[14] attributed to ring current effects.

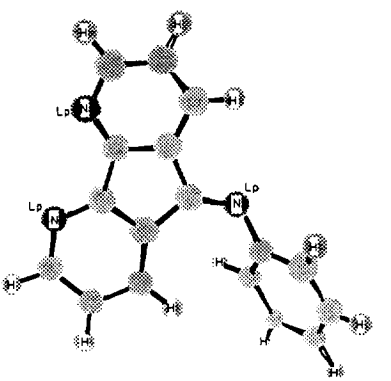

Figure 3. Structure of L_2 based on molecular modeling.

Chemical shifts for the other ligand protons behaved as expected. The chemical shift for the NH_2 protons of ligand L_1 was effected by solvent. In DMSO, the proton chemical shift was 8.93 ppm, whereas in acetonitrile it was about 7.32 ppm. The chemical shift for the hydroxy proton of the ligand L_3 overlapped with the water peak contained in the NMR solvent. The resonance of protons of the methylene group in BL_4 was a singlet with a chemical shift of about 4.12 ppm and the signal of the phenyl protons was a quartet with a chemical shift about 6.83 ppm.

UV-Visible Spectroscopy of Ligands. UV-visible spectral data are collected in Table 3 and the spectrum of BL_1 in acetonitrile is shown in Figure 4. The spectra of the ligands show three different absorption regions. The region at wavelengths longer than 310 nm have weak absorptions and are relatively well resolved. The other two regions at energies shorter than 310 nm have relatively strong absorptions. When the solvents were changed from polar to nonpolar in the series acetonitrile, methanol, chloroform, hexane, toluene, tetrachloromethane, the absorption bands remained nearly fixed, although a slight red-shift for some of the absorption bands was observed.

One strong test for distinguishing $n \rightarrow \pi^*$ transitions from $\pi \rightarrow \pi^*$ transitions is based on the effect of an oxime derivative on visible/uv spectra[15]. e.g. For benzophenone, the $n \rightarrow \pi^*$ transition disappears for its

Table 3: UV-Visible Spectral Data in Acetonitrile at Room Temperature

Ligands	λ_{max}, nm, (ε, M^{-1}, cm^{-1})		
BL_1	358(2.4×10^4), 341(2.4×10^4)	309(4.3×10^4)	240(5.8×10^4)
[a]BL_2	469[b]	317[b]	
[a]BL_3	429(1.4×10^3)		285(4.3×10^3)
BL_4	408(3.2×10^3)	313(1.5×10^4), 300((1.9×10^4)(s)	
L_1		310(1.1×10^3)	242(5.6×10^3)
L_2	398(1.3×10^3)	314(9.26×10^3), 301(1.1×10^4)	
L_3		314(9.0×10^3), 300(1.1×10^4)	270(1.2×10^4), 224(2.8×10^4)

a. In carbon tetrachloride.

b. BL_2 was not soluble enough in carbon tetrachloride to obtain a reliable extinction coefficient.

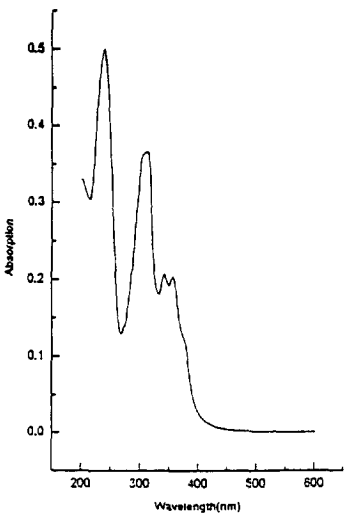

Figure 4. The UV-Visible absorption spectrum of BL_1 in acetonitrile at room temperature

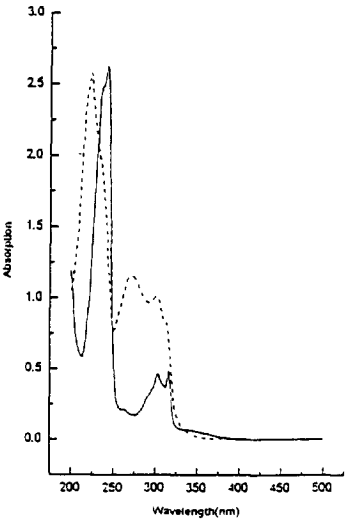

Figure 5. The absorption spectra of dafo(solid line, 2.5×10^{-5} M) and its oxime (dashed line, 5×10^{-5}M) in CH_3CN at room temperature.

oxime derivative, but produces little change in either the position or the intensity of the low-energy $\pi \rightarrow \pi^*$ transitions. Figure 5 shows the absorption spectra of 4,5-diazafluoren-9-one (dafo) and its oxime. Upon formation of the dafo oxime, no low energy absorption bands were lost nor were there changes in their position or intensity. Therefore, the low-energy transitions were assigned as $\pi \rightarrow \pi^*$ transitions.

Spectroelectrochemistry. Reduction potentials of the ligands in CH_3CN were obtained by cyclic voltammetry and differential pulse polarography. Reversibility was assessed on the basis of the oxidation/reduction peak spacings of 59/n mV, where n is the number of electrons transferred, and the ratios of i_{red}/i_{ox} which are near one for a reversible couple. The number of electrons involved in a redox process was assessed by coulometry in selected cases and then by peak area comparisons from differential pulse polarograms. The results were tabulated in Table 4.

Cyclic voltammograms of BL_1 showed two well-defined reversible reductions at $E_{1/2}$ = -0.77 V (70 mv) and $E_{1/2}$ = -1.08 V (65 mv) as illustrated in Figure 6. The n-value obtained by coulometry at -0.87 V was 0.9. Hence, both reductions are one electron processes. The BL_4 ligand showed an irreversible reduction wave

Table 4: Redox Potentials for Ligands [a]

Compounds	Oxidation $E_{1/2}$ (ΔE_p)[b]	Reductions $E_{1/2}$ (ΔE_p)[b]	
BL_1		-0.77(70)	-1.08(65)
BL_4		-0.51(irr)	-1.31(irr)
L_1	1.12(irr)		-1.58(irr)
L_2			-1.34(irr)
L_3			-1.12(irr)

a. All samples measured in 0.1 M TBAH/CH_3CN; error in potentials was ± 0.02 V; T = 23 ± 1°C; Scan rate = 200 mV/s; ΔEp in parenthesis.

b. Irr: indicates irreversible.

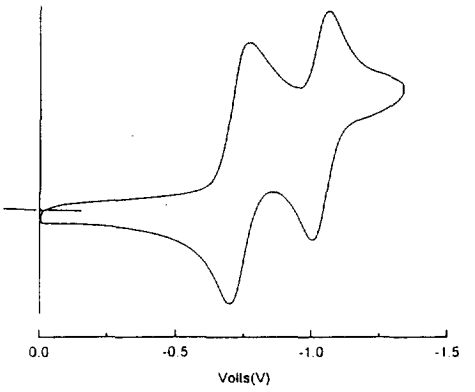

Figure 6. Cyclic voltammogram of the ligand BL_1 in acetonitrile at room temperature.

at -1.31 V and a partial return wave at -0.51 V. L_1 showed an irreversible reduction at -1.58 V and an irreversible oxidation at 1.12 V. The oxidation wave corresponds to oxidation of the NH_2 group. L_2 underwent an irreversible reduction at -1.34 V. L_3 was irreversibly reduced at -1.12 V. No electrochemical activity was detected for ligands BL_2 and BL_3 due to their low solubility in electrochemical solvents. The reduction wave, which most likely corresponds to reduction of the imine (-C=N-) group as described by Lund and Baizer[16], is common for all the ligands. The reversibility for BL_1 may be explained by the resonance structures shown in Figure 7. The partial negative charge on the carbon atom restores aromatic character to the five member rings and double reduction may stabilize the charge separation, whereas partial positive charges on neighboring nitrogen atoms is unfavorable. In this regards, a purple product that formed upon reduction of BL_1 by two electrons was stable in solution for two weeks. The peak to peak separation of BL_1 reductions was 0.31 V. However, once it is coordinated to ruthenium(II), the peak to peak separation is reduced to 0.23 V due to the presence of the positively charged metal center. This large separation is suggestive of rather strong electronic coupling between equivalent sites. This strong electronic coupling is supported by the big conproportionation constants (K_c) of 1.5 x 10^5 for (BL_1, BL_1^-) represented by the equilibria in eqs. 1 and should give rise to intervalence electron transfer (eqs. 2) in the near infrared region of the spectrum[17].

$$(BL_1^-, BL_1^-) + (BL_1, BL_1) \overset{K_c}{\rightleftharpoons} 2\,(BL_1^-, BL_1) \qquad (1)$$

$$(BL_1^-, BL_1) \overset{h\upsilon}{\rightleftharpoons} (BL_1, BL_1^-) \qquad (2)$$

The (BL_1, BL_1^-) form was generated coulometrically by reducing BL_1 at a potential midway between the first and second reductions. Details about the study of the intervalence electron transfer of BL_1 will be reported elsewhere[18].

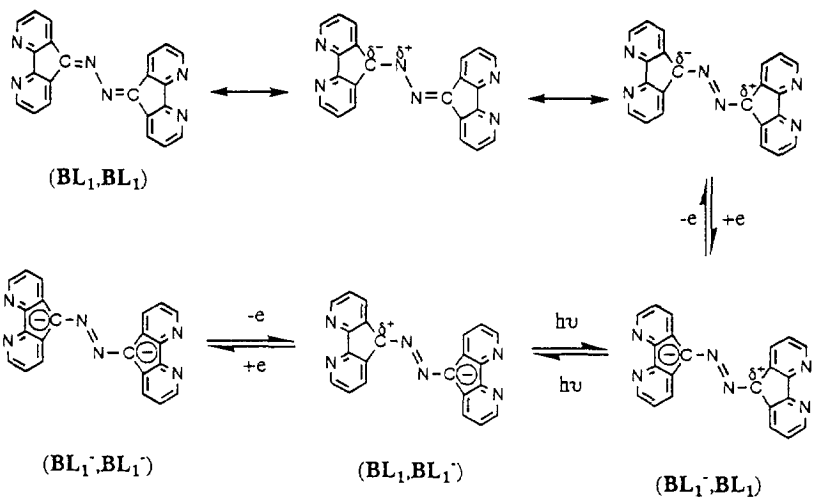

Figure 7. Resonance structures of BL_1 and its intervalence charge delocalization.

EXPERIMENTAL SECTION

Materials and Physical Measurements. All reagents and solvents were purchased commercially as HPLC grade and were used without further purification unless otherwise noted. Acetonitrile was dried over 3 Å activated molecular sieves prior to use. Commercially purchased tetrabutylammonium hexafluorophosphate (TBAH) was of electrometric grade (Southwestern Analytical, Inc.) and was used without further purification. 4,5-Diazafluoren-9-one (dafo) was prepared as described in the literature[19]. Visible-UV spectra were obtained in acetonitrile with an OLIS modified Cary 14 spectrophotometer. IR spectra were obtained in KBr pellets with

a Mattson Cynus 25 FT-IR spectrophotometer and were calibrated with the 1601 cm^{-1} band of polystyrene. ^1H NMR spectra were obtained in deuterated chloroform with a Varian XL300 spectrometer. Cyclic voltammograms and differential pulse polarograms were obtained with an EG&G PAR Model 263A potentiostat/galvanostat. Coulometry was effected using the above potentiostat and the EG&G PAR Model 377 cell system. The electrochemical measurements were made in a typical H-cell using a platinum disk working electrode, a platinum gauze counter electrode and a standard saturated sodium calomel electrode (SSCE) and digitized with an IBM 325T computer. The supporting electrolyte was 0.1 M TBAH in acetonitrile. Mass spectra were obtained with a Varian 3400 GC (SGE capillary column, BP1, 30 m) interfaced to a Finnigan Incos 50 mass spectrometer.

Preparation of L_1. The ligand was prepared using methods reported in the literature[20] and recrystallized from 1,2-dichlorobenzene. IR: 3380, 3320 and 3310 (NH), 3060 (CH ar.), 1650 and 1555 (C=N, C=C) 1420, 1200, 800 and 725 cm^{-1}. ^1H NMR ($CDCl_3$): 8.72 (d, 1 H), 8.61 (d, 1 H), 8.22 (d, 1 H), 8.13 (d, 1 H), 7.42 (dd, 1 H), 7.32 (dd, 1 H), 6.71 (broad, 2 H). Elemental analysis: Calc. for $C_{11}H_8N_4$: C, 67.32; H, 4.12; N, 28.56. Found: C, 67.22; H, 4.08; N, 28.49.

Preparation of L_2. A mixture of dafo (455 mg, 2.5 mmol), glacial acetic acid (0.15 mL, 2.5 mmol), ethanol (5 mL) and aniline (279 mg, 0.27 mL) was heated under reflux for an hour. Then, the solution was stored in a refrigerator and a bright yellow precipitate formed overnight. The solid was removed by filtration and washed with cold ethanol. The yield was 257 mg (40%). The compound was pure enough for analysis without further purification. IR: 3048 (CH, ar.), 1657, 1598, 1562, 1402 (C=N, C=C), 749 and 711 cm^{-1}. ^1H NMR ($CDCl_3$): 8.81 (d, 1 H), 8.73 (d, 1 H), 8.32 (d, 1 H), 7.41 (m, 3 H), 7.32 (t, 1 H), 7.00 (m, 3 H), 6.84 (d, 1 H). Elemental analysis: Calc. for $C_{17}H_{11}N_3$: C, 79.35; H, 4.32; N, 16.33. Found: C, 79.50; H, 4.17; N, 16.59.

Preparation of L_3. A mixture of dafo (920 mg, 5.1 mmol), hydroxylamine hydrochloride (95-98%, 520 mg, 7.5 mmol), sodium acetate (490 mg, 6.0 mmol) and water (10 mL) was heated under reflux. After about five minutes of refluxing, the mixture began to bubble vigorously. Heating was continued for 30 minutes as the froth turned yellowish. Then the mixture was placed in an ice bath. The resulting solution was suction-filtered and the solid was rinsed with cold water. The solid was recrystallized from ethanol and yielded 925 mg (92%) of product. IR: 3143 (OH), 3031 (CH, ar.), 1630, 1594, 1565, 1492, 1471 (C=N, C=C), 1000, 949 and 750

cm^{-1}. ^1H NMR ($CDCl_3$): 8.73 (m, 2 H), 8.61 (dd, 1 H), 8.22 (dd, 1 H), 7.51 (m, 2 H). Elemental analysis: Calc. for $C_{11}H_7N_3O$: C, 66.99; H, 3.59; N, 21.31. Found: C, 67.12; H, 3.80; N, 21.51 .

Preparation of BL_1. The ligand was prepared as described in the literature[18] and was recrystallized from dimethyl sulfoxide yielding red needle crystals. IR: 3060, 1630, 1590 and 1560 (C=N, C=C), 1400 and 735 cm^{-1}. ^{1}NMR ($CDCl_3$): 8.82 (d, 2H), 8.77 (d, 2H), 8.52 (d, 2H), 8.36 (d, 2H), 7.45 (dd, 2H), 7.32 (dd, 2H). Elemental analysis: Calc. for $C_{22}H_{12}N_6$: C, 73.30; H, 3.36; N, 23.32. Found: C, 73.30; H, 3.37; N, 23.35.

Preparation of $BL_2 \cdot 1/2H_2O$. A mixture of dafo (556 mg, 3.05 mmol) and 1,4-phenylenediamine (151 mg, 1.4 mmol) was refluxed in glacial acetic acid (5 mL) for an hour. After the solution was cooled to room temperature, the solid was removed by suction-filtration, washed with water, then methanol and dried under vacuum. The solid was recrystallized from nitrobenzene yielding 437 mg (70%) of red powder. IR: 1668, 1570, 1505, 1408 (C=N, C=C), 856 and 759 cm^{-1}. Elemental analysis: Calc. for $C_{28}H_{17}N_6O_{1/2}$: C, 75.45; H, 3.85; N, 18.86. Found: C, 75.56; H, 3.85; N, 18.80.

Preparation of $BL_3 \cdot 1/2H_2O$. A mixture of dafo (557 mg, 3.05 mmol) and benzidine (258 mg, 1.4 mmol) was refluxed in glacial acetic acid (5 mL) for one hour. After the solution was cooled to room temperature, the solid was removed by suction-filtration, washed with water, then methanol and dried under vacuum. The solid was recrystallized from nitrobenzene yielding 533 mg (73%) of red product. IR: 1657, 1570, 1408 (C=N, C=C), 856, 759 cm^{-1}. ^1H NMR (CD_3SOCD_3): 8.81 (d, 2H), 8.66 (d, 2H), 8.26 (d, 2H), 7.78 (d, 4H), 7.40 (dd, 2H), 7.12 (d, 6H), 7.02 (dd, 2H). Elemental analysis: Calc. for $C_{34}H_{21}N_6O_{1/2}$: C, 78.28; H, 4.06; N, 16.12. Found: C, 78.08; H, 4.41; N, 16.09.

Preparation of $BL_4 \cdot 1/2CH_3OH$. A mixture of dafo (556 mg, 3.05 mmol) and 4,4'-methylenedianiline (278 mg, 1.4 mmol) was refluxed in glacial acetic acid (5 mL) for 0.5 h. After the solvent was removed by rotary evaporation, 5 mL methanol was added and the solid was removed by vacuum filtration, washed with methanol and finally ether. The solid was recrystallized from methanol yielding 509 mg (67%) of product. IR: 1655, 1593, 1560, 1498, 1400 (C=N, C=C), 856, 759 cm^{-1}. Elemental analysis: Calc. for $C_{36}H_{24}N_6O_{1/2}$: C, 78.57; H, 4.46; N, 15.49. Found: C, 78.60; H, 4.50; N, 15.72.

CONCLUSIONS

4,5-Diazafluorenone has proven to be a versatile building block for construction of polypyridyl bridged ligands. Long-range ring current effects in the proton NMR was observed among these ligands. Absorption bands were assigned as $\pi \rightarrow \pi^*$ transitions. A test for $n \rightarrow \pi^*$ transitions, based on the effect of oxime formation on the absorption spectra rule out such transitions. Molecular ion peaks in the mass spectra of these ligands were consistent with their formulation and also indicated the stability of the ligands in the gas phase were in the order: $BL_2 > BL_1 > BL_3 > BL_4$. The ligands were all irreversibly reduced, except for BL_1 where two well-defined reversible, one-electron reductions were found.

ACKNOWLEDGMENT

The authors thank the Office of Basic Energy Sciences of the United States Department of Energy for support.

REFERENCES

1. (a) Woitelier, S; Launay, J.-P. *Inorg. Chem.* **1989**, *28*, 758-762. (b) Joachim, C.; Launary, J. P.; Woitellier, S. *Chem. Phys.* **1990**, *147*, 131-141. (c) Ribou, A. C.; Launay, J. P.; Takahashi, K.; Nihira, T.; Tarutani, S.; Spangler, C. W. *Inorg. Chem.* **1994**, *33*, 1325-1329. (d) Collin, J. P.; Laine, P.; Launay, J. P.; Sauvage, J. P.; Sour, A. *J. Chem. Soc., Chem. Commun.* **1993**, 434-435.

2. (a) Balzani, V., Ed.*Supramolecular Photochemistry* ; NATO ASI series, D. Reidel Publishing Company, 1987. (b) Meyer, T. J. *Acc. Chem. Res.* **1989**, *22*, 163-170. (c) Balzani, V., Scandola, F., Eds.,*Supramolecular Photochemistry*; Horwood: Chichester, U. K., 1990.

3. (a) Juris, A.; Balzani, V.; Barigelletti, F.; Campagna, S.; Belser, P.; Von Zelewsky, A. *Coord. Chem. Rev.* **1988**, *84*, 85-277. (b) Ward, M. D. *Chem. Soc. Rev.* **1995**, 121-134. (c) DeArmond, M. K.; Carlin, C. M. *Coord. Chem. Rev.* **1981**, *36*, 325-355.

4. (a) Bignozzi, C. A.; Roffia, S.; Chiorboli, C.; Davila, J.; Indelli, M. T.; Scandola, F. *Inorg. Chem.* **1989**, *28*, 4350-4358. (b) Curtis, J. C.; Bernstein, J. S.; Meyer, T. J. *Inorg. Chem.* **1985**, *24*, 385-397. (c) Schmehl, R. H.; Auerbach, R. A.; Wacholtz, W. F.; Elliot, C. M.; Freitag, R. A.; Merkert, J. W. *Inorg. Chem.* **1986**, *25*, 2440-2445. (d) Ohno, T.; Nozaki, K.; Haga, M. *Inorg. Chem.* **1992**, *31*. 4256-4261.

5. (a) Ward, M. D. *Chem. Soc. Rev.* **1995**, 121-134. (b) Kalyanasundaram, K.; Nazeeruddin, M. K. *Inorg. Chim. Acta* **1994**, *226*, 213-230.

6. Sauvage, J. P.; Collin, J. P.; Chambron, J. C.; Guillerez, S.; Coudret, C.; Balzani, V.; Barigelletti, F.; De Cola, L.; Flamigni, L. *Chem. Rev.* **1994**, *94*, 993-1019.

7. (a) Kahn, O.; *Molecular Magnestism*; VCH Publishers, Inc.: New York, 1993. (b) Das, A.; Maher, J. P.; McCleverty, J. A.; Navas badiola, J. A.; Ward, M. D. *J. Chem. Soc. Dalton Trans.* **1993**, 681-686.

8. (a) Strouse, G. F., Schoonover, J. R., Duesing, R., Boyde, S.; Jones, W. E. Jr.; Meyer, T. J. *Inorg. Chem.* **1995**, *34*, 473-487. (b). Baba, A. I.; Ensley, H. E., Schmehl; R. H. *Inorg. Chem.* **1995**, *34*, 1198-1207.

9. (a) Song, X.; Lei, Y.; Van Wallendael, S.; Perkovic, M. W.; Jackman, D. C.; Endicott, J. F.; Rillema, D. P. *J. Phys. Chem.* **1993**, *97*, 3225-3236; (b) Sahai, R.; Baucom, D. A.; Rillema, D. P.; *Inorg. Chem.* **1986**, *25*, 3843-3848; (c) Larson, S. L.; Hendrickson, S. M.; Ferrere, S.; Derr, D. L.; Elliott, C. M. *J. Am. Chem. Soc.* **1995**, *117*, 5881-5882; (d) Furue, M.; Kuroda, N.; Sano, S. J. *Macromol. Sci. Chem.* **1988**, *A25*, 1263-1266.

10. Wang, Y.; Jackman, D. C.; Woods, C.; Rillema, D. P. *J. Chem. Crystallog.* **1995**, *25*, 549-553.

11. Karbatsos, G. J. and Osborne, C. E. *Tetrahedron*, **1968**, 24, 3361-3368.

12. Minabe, M., Takabayashi, Y., Setta, Y., Nakamura, H., Kimura, T., and Tsubota, M. *Bull. Chem. Soc. Jpn.*, **1996**, 69, 3633-3638.

13. Drago R. S. *Physical Methods for Chemists.*; 2nd Ed; Saunders College Publishing: New York, **1992**.

14. Abraham, R. J.; Fisher, J.; Loftus, P. *Introduction to NMR Spectroscopy* ; John Wiley & Sons Ltd: New York, **1988**.

15. Yoshihard Keitaro, Kearns, D. R., *J. Chem. Phys.* **1966**, *45*, 1991-1999.

16. Lund H, Baizer, M. M., *Organic Electrochemistry: An Introduction and A Guide*; 3rd ed.; Marcel Dekker, Inc., New York, **1991**.

17. Brown, D. B., *Mixed-Valence Compounds: Theory and Applications in Chemistry, Physics, Geology, and Biology*, D. Reidel Publishing Company, **1979**.

18. Wang, Y.; Rillema, D. P., submitted to *J. Chem. Soc. Chem. Commun.*

19. Henderson, L. J.; Fronczek, Jr., F. R.; Cherry, W. R. *J. Am. Chem. Soc.* **1984**, *106*, 5876-5879.

20. Mlochowski, J., Szule, Z. *Pol. J. Chem.* **1983**, *57*, 33-39.

(*Received in USA* 10 *February* 1997; *revised* 23 *June* 1997; *accepted* 4 *July* 1997)